J Math Chem (2012) 50:2689–2702
DOI 10.1007/s10910-012-0058-y

ORIGINAL PAPER

On characterizing proteomics maps by using weighted Voronoi maps

Rok Orel · Milan Randić

Received: 5 February 2012 / Accepted: 14 July 2012 / Published online: 31 July 2012

Abstract In contrast to the standard construction of Voronoi regions, in which the boundaries between different regions are at equal distance from the given points, we consider the construction of modified Voronoi regions obtained by giving greater weights to spots reported to have higher abundance. Specifically we are interested in applying this approach to 2-D proteomics maps and their numerical characterization. As will be seen, the boundaries of the weighted Voronoi regions are sensitive to the relative abundances of the protein spots and thus the abundances of protein spots, the z component of the (x, y, z) triplet, are automatically incorporated in the numerical analysis of the adjacency matrix, rather than used to augment the adjacency matrix as non-zero diagonal matrix elements. The outlined approach is general and it may be of interest for numerical analyses of other maps that are defined by triplets (x, y, z) as input information.

Keywords Proteomics maps · Voronoi regions · LY171833 peroxisome proliferator · Weighted Voronoi regions

1 Introduction

We consider a novel representation of proteomics maps, which are characterized by a triplet of numbers (x, y, z), where (x, y) give the locations of the proteins and the

R. Orel
XLAB, Pot za Brdom 100, Ljubljana, Slovenia
e-mail: rok.orel@xlab.si

M. Randić (✉)
National Institute of Chemistry, Hajdrihova 19, Ljubljana, Slovenia
e-mail: mrandic@msn.com

coordinate z the abundance. The resulting 2D maps incorporate indirectly information on protein abundances. The outlined approach, which is general and applies equally to other problems involving triplets of numbers (x, y, z), illustrates a novel route to 2D graphical representation of 3D geometrical objects distinct from approaches using traditional projections.

After a brief review of several approaches to the numerical characterization of proteomics maps, we will outline the construction of the adjacency matrix for proteomics maps for a set of N points having known (x, y) coordinates based on boundaries of accompanying Voronoi regions. A description of earlier developments on numerical characterization of proteomics maps can be found in a review [1]. More recent developments relating to numerical characterization of proteomics maps have been outlined in other reviews [2,3]. All hitherto approaches, including also one based on Voronoi regions [4], initially ignore the abundances of protein spots (the third coordinate of a straightforward 3D representation of such maps). After one constructs matrices associated with the representation of the map as a geometrical object, the information of the relative abundances is taken into account by replacing the diagonal zeros with abundance values.

Matrices hitherto considered were the adjacency (A) and the distance (D) matrix of a graph superimposed over a proteomics map. The former is a *sparse* matrix (matrix having many off-diagonal zero entries) whereas the latter is *dense* matrix (matrix with non-zero numerical off-diagonal matrix elements), which are computationally more intense. In addition one can also consider a hybrid matrix, the adjacency-distance matrix AD, in which one considers only distances between adjacent spots, or adjacent spot regions. In the case of maps based on Voronoi regions, the AD matrix is constructed by replacing the binary elements A(i, j) of the adjacency matrix by the corresponding numerical elements of the distance matrix D(i, j), given by the distance between the center spots of the corresponding regions. We should also mention the D/D matrix [5], the matrix elements of which are given as the quotients of the Euclidean distance and the distance along the shortest path connecting the pair of points in (x, y) plane.

The abundances of spots are incorporated as diagonal entries of such matrices after suitable weighting of abundances. A similar *ad hoc* approach has been used to differentiate among heteroatoms in molecular graphs, leading to variable connectivity indices for use in SAR and QSAR studies [6–8]. Here we will outline a different way to incorporate the information on abundances of spots in a proteomics map into matrices to represent proteomics maps. The basis for this novel approach is our observation that the introduction of weighting factors (that depend on the relative values of the abundances) causes Voronoi regions to change their boundaries. Consequently one arrives at variations of adjacency matrices or map regions, that is variations in off-diagonal elements of adjacency matrices.

After an introductory outline on numerical characterization of proteomics maps we will describe the new approach and will illustrate it on a set of proteomics maps using different concentrations of the same peroxisome proliferator administrated of to experimental animals. The data used for illustration is that of Anderson et al. [9], the proteomics maps of which has been analyzed by principal component analysis by Anderson et al. [9], and a graph theoretical approach [10,11] in the which no infor-

mation on (x, y) coordinates was used. The (x, y) coordinates are of interest when comparing proteomics maps, but are irrelevant when one wishes to compare proteomes (collection of proteins in a single cell). Significantly, despite using different inputs both graph-theoretical approaches eventually have shown the presence of hormesis at the cellular level (that is a non-linear dose-response curve). Thus while the hormesis at the cellular level is not in question, it remains of considerable interest to see which theoretical approaches can also confirm this spectacular result, which Anderson et al., who used the principal component analysis, could not detect.

2 Numerical representation of proteomics maps

A way to arrive at a matrix to represent proteomics map is to associate with any proteomics map some geometrical object. The first numerical characterization of proteomics maps was obtained by simply connecting (by line segments) spots in a map in sequential order of their relative abundances [12–14]. This produced a zigzag curve for which one can construct D and D/D matrices. It is also possible to construct alternative zigzag curves based on the ordering of protein spots relative to their charges and relative to their mass [15], or based on canonical labels for protein spots [16]. Another approach is to consider partial ordering for protein spots, using the coordinates (x, y) of spots as entries for a graph depicting partial order [17,18]. The partial ordering thus induces a graph having fixed geometry embedded over the map, the adjacency matrix of which is the starting point for evaluating selection of graph invariants as map descriptors. Later on, additional graph embeddings over the proteomics map were constructed: (i) by clustering spots at distances shorter than a selected critical distance [19]; (ii) by connecting spots which form the nearest neighbors [20], and more recently (iii) by construction of the graph embedded over the proteomics map obtained by connecting spots 1 and 2 and then connecting each successive spot to the nearest spot having the smallest label [21,22]. Such a construction has an advantage in that if one decides to augment the map by introducing additional spots, the resulting tree (acyclic graph) will be an extension of the existing graph. In other words, new vertices will be added to the already constructed tree, which will remain the same; this is not the case if one is to connect spots which form the nearest neighbors.

What is common to all these approaches is that they allow one to construct matrices A, D, AD and D/D, the selected invariants of which (like for example the leading eigenvalues, the set of eigenvalues, the coefficients of the characteristic polynomials, the average matrix elements, the ordered set of row sums, and such) allow one to make numerical comparisons of different maps. However, before such comparisons can be meaningful, one has to modify the A, D, AD and D/D matrices to include the information on relative abundances. In proteomics maps of the same living cells subject to different procedures proteins always have the same (x, y) coordinates (they do not change mass or charge) so such maps differ only by showing different abundances. A way to include abundances, as already mentioned, is to replace zeros on the main diagonal by the values of suitably scaled abundances as the diagonal matrix elements. The scaling of the diagonal elements allows one to adjust and give a greater or lesser role to diagonal entries in a matrix. If one has no special reasons to do differently, it

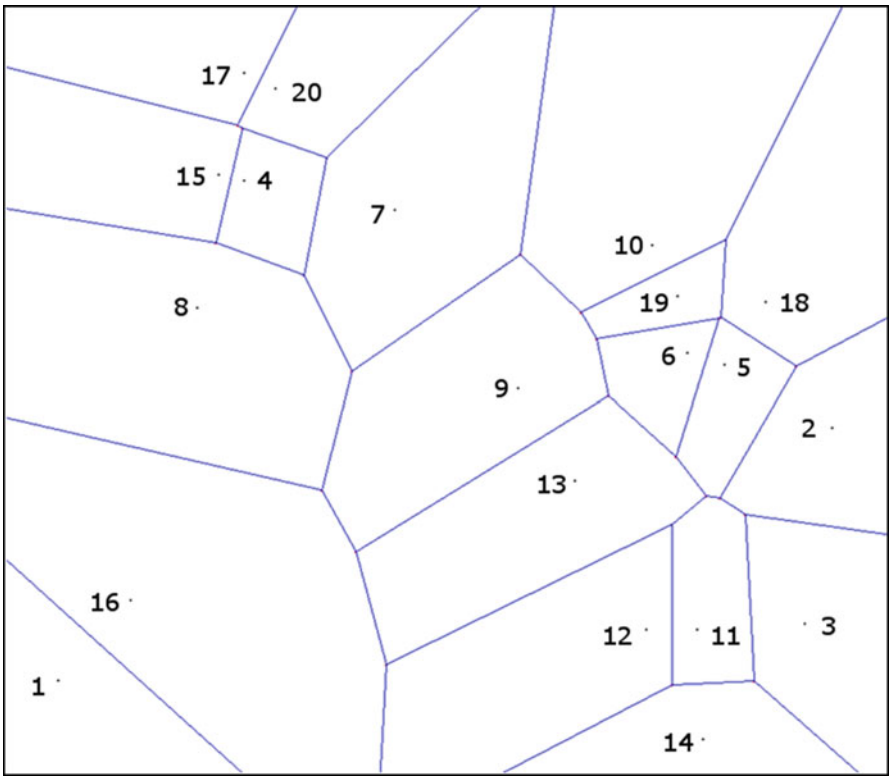

Fig. 1 Voronoi regions for the 20 most abundant protein spots of the protomics maps of mice liver cells as reported by Anderson et al. [7] for the control group of animal

was recommended that diagonal entries are scaled so that the sum of diagonal entries is the same as the sum of off-diagonal entries [18].

3 Partitioning of maps into Voronoi regions

Recently in this journal we have outlined a scheme for arriving at numerical characterizations of proteomics maps by partitioning of proteomics map into Voronoi regions [23]. About 100 years ago, in 1907, the Russian mathematician Voronoi outlined a general procedure for partitioning of a plane in which there are N points with coordinates (x_i, y_i) $(i = 1, 2, 3, \ldots N)$ into N regions such that each region R_i consists of all points (x, y) of the plane which are closer to point i than any other point $j \neq i$ [24]. For a thus-partitioned plane, one can construct the adjacency matrix A, the corresponding distance matrix D, the adjacency-distance matrix AD, and the distance/distance matrix DD. In Fig. 1 we illustrate, for a proteomics map of mouse liver cells, Voronoi regions for 20 spots having the largest abundances. This is the proteomics map for the control group in a study of the effects of peroxisome proliferators on protein abundances in mouse liver cells carried out by Anderson et al. [9]. Table 1, columns two and three,

Table 1 The coordinates of 20 spots of proteomics map having the largers abundance for the control group

Spot	Coordinates		Control	Concentration of LY171883					
	x	*y*	0	0.003	0.01	0.03	0.1	0.3	0.6
1	−0.198	−0.192	0.464	0.515	0.455	0.502	0.498	0.578	0.394
2	0.198	−0.063	0.438	0.402	0.522	0.425	0.371	0.181	0.198
3	0.184	−0.163	0.353	0.467	0.385	0.304	0.422	0.313	0.295
4	−0.103	0.063	0.251	0.203	0.248	0.275	0.272	0.353	0.424
5	0.143	−0.031	0.190	0.108	0.141	0.184	0.104	0.138	0.150
6	0.124	−0.025	0.182	0.168	0.158	0.151	0.149	0.131	0.114
7	−0.026	0.048	0.171	0.157	0.081	0.093	0.139	0.097	0.050
8	−0.127	−0.002	0.138	0.073	0.080	0.091	0.110	0.073	0.128
9	0.037	−0.043	0.134	0.088	0.114	0.108	0.127	0.070	0.076
10	0.106	0.030	0.126	0.116	0.107	0.102	0.100	0.106	0.070
11	0.129	−0.166	0.100	0.137	0.069	0.079	0.060	0.065	0.010
12	0.103	−0.166	0.090	0.111	0.061	0.054	0.052	0.056	0.005
13	0.066	−0.090	0.088	0.054	0.059	0.052	0.067	0.038	0.022
14	0.132	−0.222	0.083	0.077	0.070	0.080	0.063	0.067	0.055
15	−0.116	0.066	0.083	0.063	0.069	0.079	0.093	0.099	0.126
16	−0.161	−0.151	0.078	0.059	0.037	0.044	0.058	0.062	0.050
17	−0.103	0.118	0.072	0.054	0.099	0.127	0.168	0.208	0.295
18	0.164	0.001	0.069	0.051	0.122	0.109	0.092	0.143	0.205
19	0.119	0.004	0.068	0.051	0.069	0.079	0.078	0.098	0.106
20	−0.087	0.110	0.029	0.036	0.040	0.038	0.036	0.040	0.054

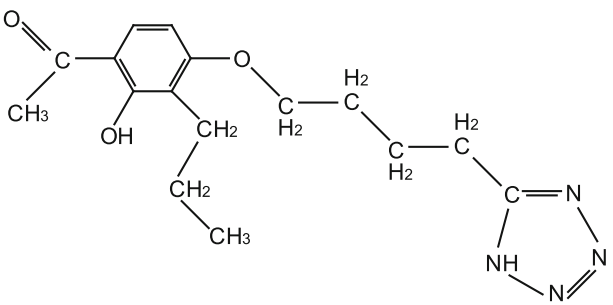

Fig. 2 The peroxisome proliferator LY171883

list the x, y coordinates for the selected 20 spots, whereas in the following columns are listed the corresponding abundances. The remaining columns of Table 1 give the corresponding abundances for the selected 20 protein spots for animals exposed to various concentrations of the peroxisome proliferator LY171883, illustrated in Fig. 2, the proteomics maps of which we will later examine thoroughly.

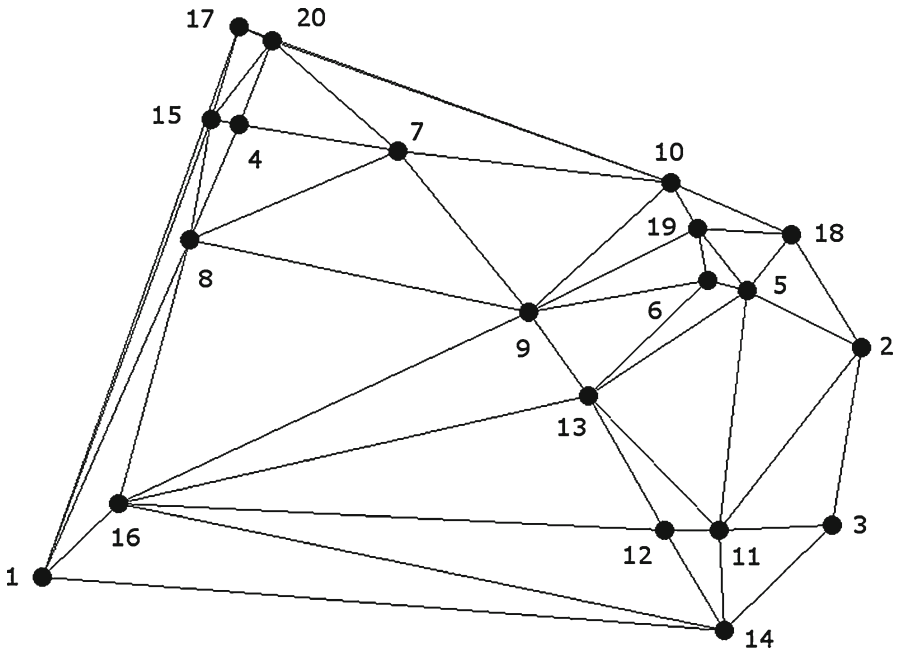

Fig. 3 The Delaunay triangulation, the dual of Voronoi regions of Fig. 1

Observe that Fig. 1 is truncated, but in fact it extends to infinity. We call adjacent the regions sharing a border of non-zero length. The adjacency and the boundaries between some regions on the periphery of the finite image need not be obvious. For example, while one can deduce that regions 1 and 8 are adjacent, and even that regions 10 and 20 may be adjacent, it is not clear if region 1 is adjacent to region 3. It looks that region 1 is not adjacent to region 17, but whether region 1 and region 3 are adjacent is much harder to decide by visual examinations of the finite part of the (x, y) plane. Fortunately, there is a way to establish the adjacency for various regions on the boundary of truncated Voronoi map outlined by Delaunay [25]. Already in 1934 Delaunay, a student of Voronoi, has shown that the construction of a dual of Voronoi map which is illustrated in Fig. 3 for the map of Fig. 1 gives an answer on adjacency of Voronoi regions. Geometrically speaking, Fig. 3, which is the dual of Voronoi map, represents the triangulation of the map of Fig. 1.

The adjacency matrix of the graph of Fig. 2 has zeros on the main diagonal, which is used to incorporate suitably scaled abundances of the 20 spots of Table 1 (fourth column). In Ref. [18] we have outlined how the abundances of spots should be scaled before being inserted as the diagonal elements to the augmented adjacency matrix. According to Kowalski and Bender [26] such input data (experimental x, y, z quantities which may be of different nature and measured by different units) should be rescaled to the interval [0, 1]. However, it was argued in ref. [16] that in our approach this is not adequate because (x, y) represent off-diagonal elements of matrices while abundances define the diagonal matrix elements. The rescaling by Kowalski and Bender does not

take into account the *size* of the adjacency matrix, which in our case plays a role. For example, scaling of diagonal entries for 20 proteins of the 20×20 adjacency matrix in order to balance the influence of non-diagonal entries will not hold when one considers 40 proteins, because in the 40×40 adjacency matrix the off-diagonal matrix elements would outweigh the role of the diagonal elements of a 20×20 matrix. A way out is to normalize diagonal entries of a matrix so that the sum of diagonal entries equals the sum of off-diagonal entries in the matrix. This procedure allows an extension of analysis by inclusion of larger number of protein spots in proteomics maps. Knowing all these preliminary steps, we decided in this article to reconsider Voronoi diagrams by taking the abundances as the weighting factors in partitioning of the (x, y) plane so that regions belonging to spots having larger abundance receive a proportionally larger share of space as compared to traditional partitions in which all points in plane have the same weight.

4 Partition of the plane into Voronoi regions by weighted protein spots

The rule for partition of a plane having N points with coordinates (x_i, y_i) $(i = 1, 2, 3, \ldots N)$ into Voronoi regions states that each region contains all points in the plane nearest to one of the N points with coordinates (x_i, y_i). Let us use the symbol D_i for the distance of any point (x, y) in a plane from point (x_i, y_i), and D_{ii} for the abundance of the spot with coordinates (x_i, y_i). We will use a modified rule for Voronoi regions partitioning of the plane into "Weighted Voronoi Regions" [27]:

> All points in the plane for which the product $D_i D_{ii}$ is the smallest define the weighted Voronoi region for point (x_i, y_i).

In Fig. 4 we illustrate the map of weighted Voronoi regions for the same 20 spots with the largest abundance for the control group of the proteomics map of mouse liver cells from the study of Anderson et al. [7]. This figure was drawn using the available multiplicatively weighted Voronoi diagram, computer program of Mu [28]. As was the case with Fig. 1 also Fig. 4 is truncated, and in fact it extends to infinity. Here again there may be difficulties to determine adjacencies for some regions; although most regions are determined by curves, this appears less troublesome. Possible uncertainties appear when four curves appear to meet in a single point, as may be the case with regions 1, 4, 7, and 9. This will not happen often but while in such cases a higher resolution of the figure may give the answer, it is better again to construct the dual of the Voronoi diagram, which we have illustrated in Fig. 5. As we see from Fig. 5, the region 1 and the region 7 are not adjacent, because the corresponding vertices of the graph are not connected.

Observe that now the dual of the Voronoi diagram could be a non-planar graph, i. e. a graph exhibiting crossing of lines, as is the case with the lines connecting the pair 7, 9 and the pair 2, 4. In addition the dual or Delaunay diagram, no longer represents a triangulation of Voronoi diagram as there are many terminal vertices (corresponding to isolated regions) and bridge vertices (like the spots 8 and 13 in Fig. 5). However, the graph allows the construction of the adjacency matrix and other matrices of interest and thus serves a useful purpose. A comparison of Figs. 1 and 4 does not appear to

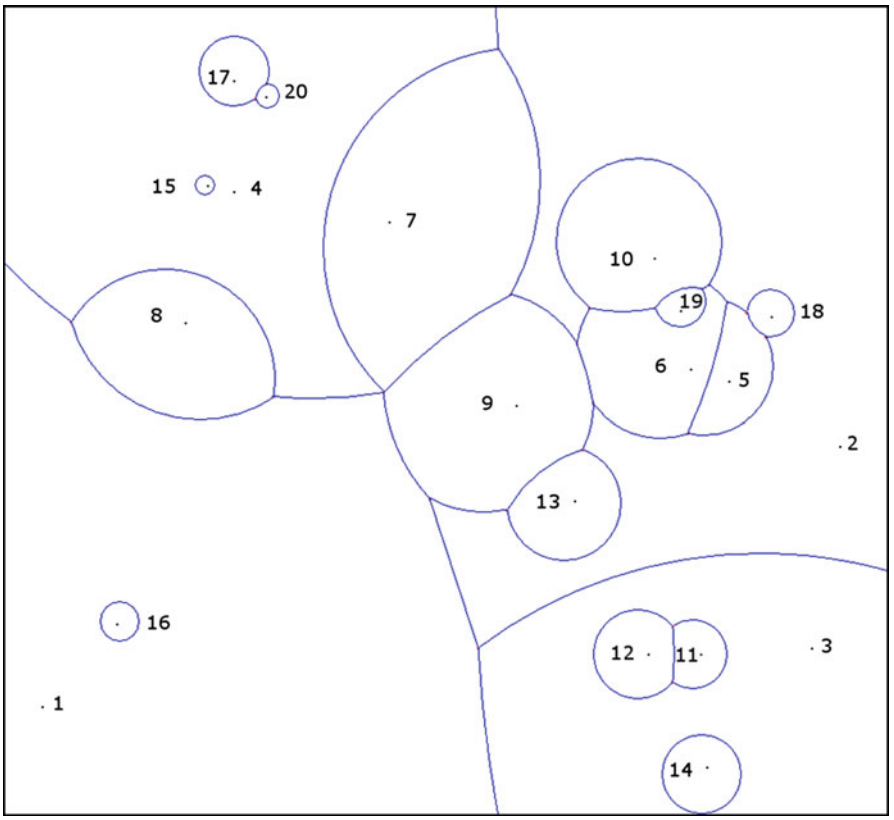

Fig. 4 Voronoi regions for the 20 most abundant protein spots of the protomics maps of mice liver cells as reported by Anderson et al. [7] for the control group of animals

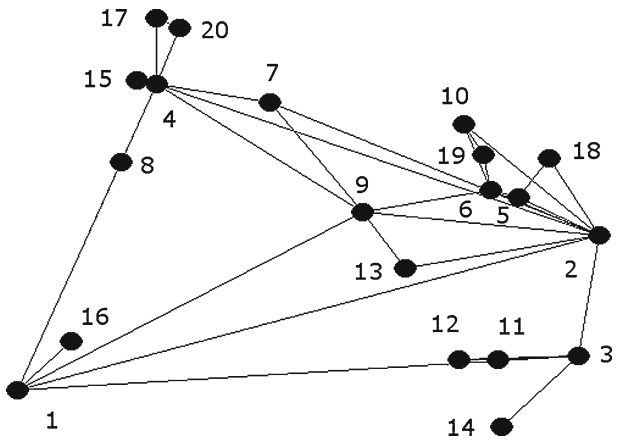

Fig. 5 The Delaunay dual of Voronoi regions of Fig. 4

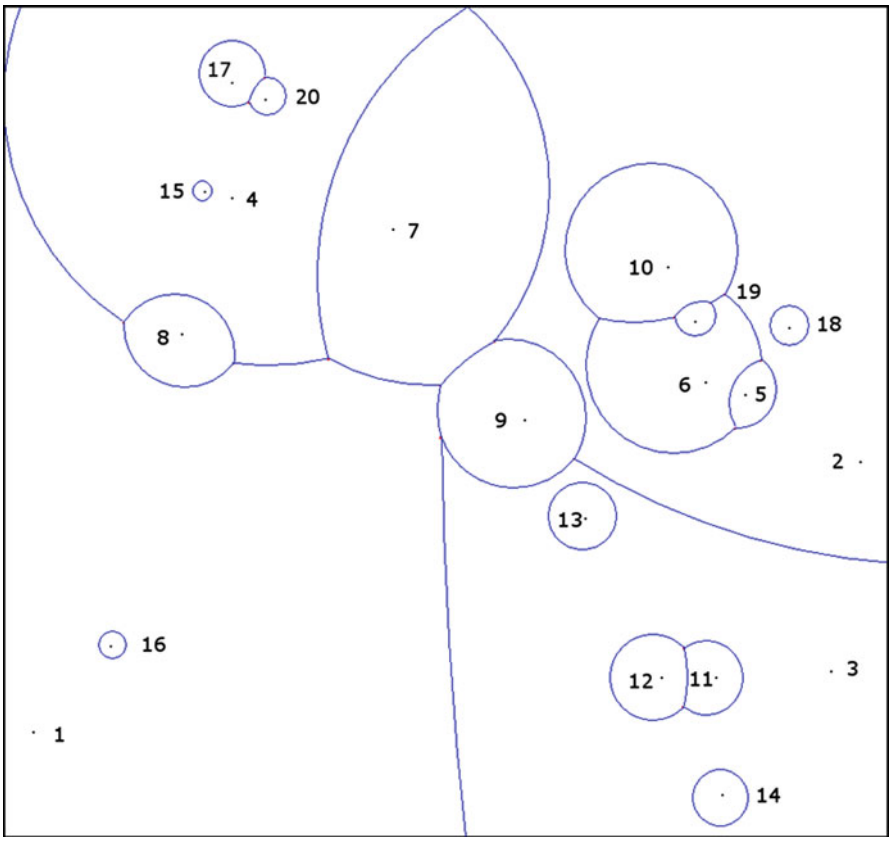

Fig. 6 Voronoi regions for the 20 most abundant protein spots of the protomics maps of mice liver cells as reported by Anderson et al. [7] for the concentration of 0.003 of LY171883 in animal food

offer useful insights, because the two Voronoi diagrams are vastly different. Similarly a comparison of Fig. 3 with Fig. 5 of the corresponding Delaunay diagrams equally does not give useful insights because the two diagrams are again vastly different. Not only that the Delaunay diagram of weighted regions has many missing lines that are present in Fig. 3, but it also has lines that are not present in the diagram of Fig. 3, such as the connections (1, 2), (1, 3), and (1, 9), then (2, 6), (2, 4), (2, 9) and (2, 13) and so on.

The situation appears chaotic, but as we will see, this is not a cause for desperation, but it may be viewed as a blessing in disguise. What that means is that the diagrams of Figs. 3 and 5 have vastly *different* adjacency matrices, and in this approach the information on the relative abundances of protein spots are directly reflected by *changes* in the adjacency matrices. We may conclude that in the construction of weighted Voronoi regions, the abundance of the protein spots in the proteomics maps is only one of contributing factors, and one no longer needs to use diagonal elements of the adjacency matrix to include information on the third coordinate of the triple (x, y, z). This is a profound novelty as it illustrates how data from a 3D space, which is the

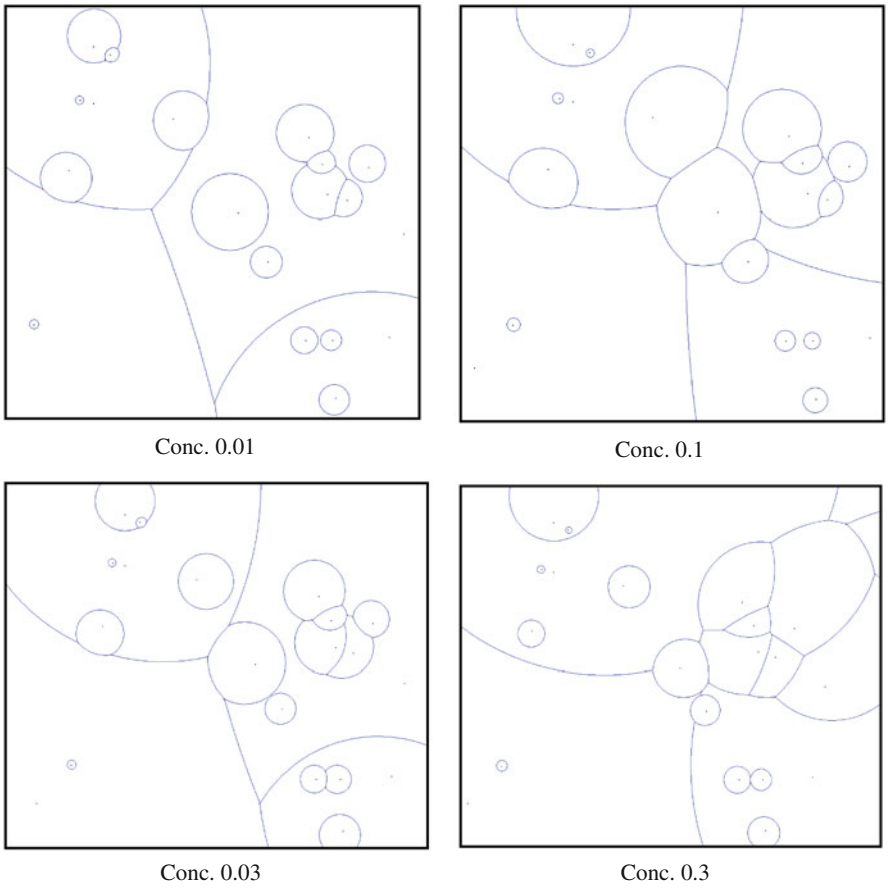

Fig. 7 Voronoi regions for the 20 most abundant protein spots of the protomics maps of mice liver cells as reported by Anderson et al. [7] for the concentration of 0.003 of LY171883 in animal food

natural space for depicting triplets (x, y, z), can in some situation, as is one illustrated here, be reduced to visual information in 2D space. This for itself would be enough to advertise this novelty, but since we are interested in further developments of numerical characterizations of proteomics maps we will continue to explore this novel approach in order to see if it can be of help in analyzing of experimental data of proteomics maps and in showing possible hidden features of such maps.

5 Use of weighted Voronoi regions for analyzing a set of related proteomics maps

We decided to revisit the data of Anderson et al. [7], who investigated effects of peroxisome proliferators on protein abundances in mouse liver, and reported on variations in abundances of liver cell proteins under variation of peroxisome proliferator LY171883

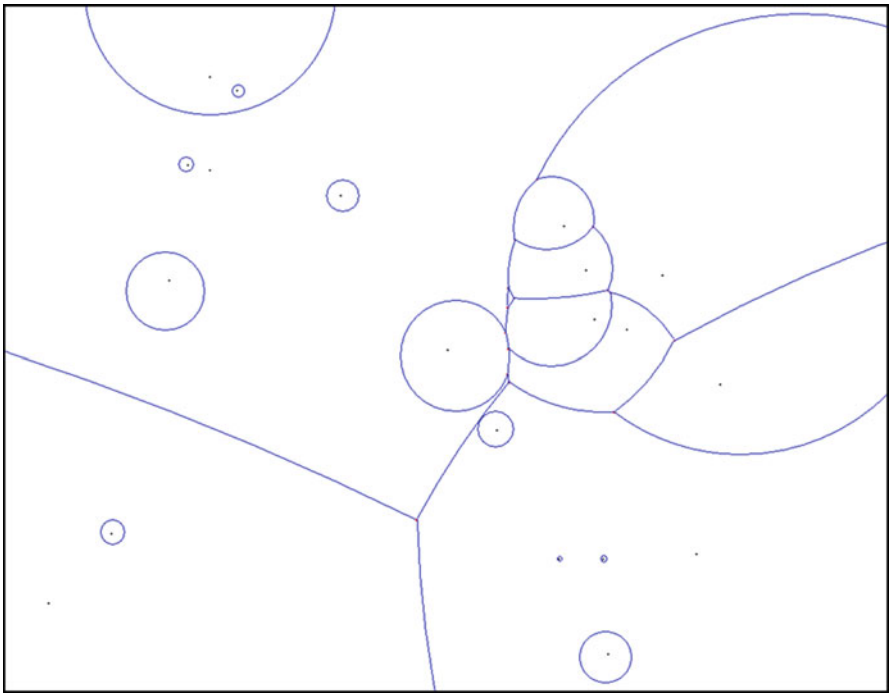

Fig. 8 Weighted Voronoi diagram for the maximal of LY171883 concentration of 0.6 in mice food

with gradual change of concentration of LY171883 from 0.003 to 0.6 (a total of six concentration steps). A few years ago, Randić and Estrada [11] examined their results but focused the attention solely to abundances, ignoring the information on the (x, y) coordinates (that define the proteomics maps, but are irrelevant for the cell proteome). In doing this, they were able to observe a J-shaped dose-response curve, typical of hormesis, thus demonstrating for the first time hormesis at the cellular level. A few years later by re-examining an earlier graph in a theoretical characterization of proteomics maps by Randić et al. [21] it was found the same J-shaped dose-response curve, which was thus hidden in proteomics map data but was not recognized at that time, 2 years before the paper of Randić and Estrada [11], and was only rediscovered around 7 years later, when writing a review article on graphical representation of proteins, published in *Chemical Reviews* [2]. It is of interest therefore to see if this novel approach to abundances in proteomics maps will lead to similar results as reported in refs. [2,11], which we will examine in this section of the article.

In Fig. 6 we show the map of the multiplicatively weighted Voronoi diagram for LY171883 concentration 0.003, the smallest concentration used in the experiment of Andersen at al. It is interesting to compare this diagram with that of the control group, shown in Fig. 4. It is pleasing to see that the two diagrams are very similar, even though, when one looks to details, there are significant differences. A comparison of Figs. 4 and 6 shows that the approach using weighted Voronoi regions appears to be sound and in no way chaotic. Though the changes between the two maps are small,

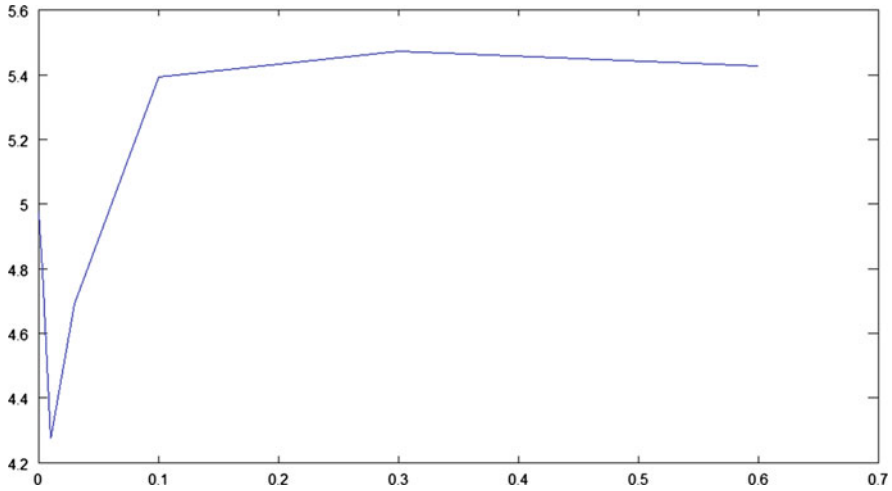

Fig. 9 Plot of the leading eigenvalue of the adjacency matrices of weighted Voronoi regions against the concentration of LY171883 in mice food

they are sufficient to alter several adjacency relationships. Thus the spots 13 and 18 became isolated, while the adjacency of the regions 6 and 9 was disrupted. On the other hand, regions 1 and 7 that were disjoint in the map of the control group, are now adjacent. Briefly, all this is a consequence of changes in abundances of the spots after a very small dose of LY171883 was introduced into animal food.

In Fig. 7 we show the maps of weighted Voronoi diagrams for LY171883 for concentrations of 0.01, 0.03, 0.1 and 0.3 and in Fig. 8 is the diagram for the maximal concentration of 0.6 of LY171883 in mice food. Observe that gradual change of the concentration makes gradual changes in Voronoi diagrams that allow one to follow the changes, but the last two steps are larger and so are the changes in the Voronoi diagrams.

In conclusion we may say that while the abundances in proteomics maps change chaotically (that is, in a non-predictive manner) the differences in maps for in-between cases are not chaotic and allow one to identify regions of the diagram without many difficulties. The maps allow one to see which spots have increased, decreased or even drastically increased or decreased their abundance as concentrations varied. Thus clearly adjacency matrices of weighted Voronoi regions are sensitive to variations in abundances of different spots. However, of prime interest is to see whether such changes are reflected in changes in selected matrix invariants that may tell us something about the trends in otherwise apparently chaotic variations of individual spot abundances with changes in concentrations of LY 171883.

In order to see if the already observed hormesis at the proteome cell level can be detected by this new approach, we calculated the leading eigenvalue (λ_1) of the novel 20×20 adjacency matrices which are listed bellow:

Conc.	0	0.003	0.01	0.03	0.1	0.3	0.6
λ_1	4.978	4.796	4.272	4.692	5.392	5.473	5.429

The graphical representation of the variation of the leading value of the adjacency matrix of weighted Voronoi regions versus concentration is shown in Fig. 9. This result is pleasing as it agrees with the two previously reported dose-response curves, particularly as the three approaches, this one included, are based on related but distinct theoretical models.

Acknowledgments RO thanks for financial support the European Union, European Social Fund. MR would like to thank the Laboratory for Chemometrics, National Institute of Chemistry, Ljubljana, Slovenia, for hospitality and partial financial support. This work has been supported in part by the Ministry of Science and Higher Education, of Republic of Slovenia under Research Grant P1017.

References

1. M. Randić, in *Quantitative Characterization of Proteomics Maps by Matrix Invariants*, ed. by P.M. Conn. Handbook of Proteomics Methods (Humana Press, Inc., Totowa, NJ, 2003), pp. 429–450
2. M. Randić, J. Zupan, A.T. Balaban, D. Vikić-Topić, D. Plavšić, Graphical representation of proteins. Chem. Rev. **111**, 790–862 (2011)
3. H. González-Díaz, Y. González-Díaz, L. Santana, F.M. Ubeira, E. Uriarte, Proteomics, networks and connectivity indices. Proteomics **8**, 750–778 (2008)
4. M. Randić, R. Orel, On numerical characterization of proteomics maps based on partitioning of 2-D maps into Voronoi regions. J. Math. Chem. **49**, 1759–1768 (2011)
5. M. Randić, A.F. Kleiner, L.M. DeAlba, Distance/distance matrices. J. Chem. Inf. Comput. Sci. **34**, 277–286 (1994)
6. M. Randić, Novel graph theoretical approach to heteroatom in quantitative structure-activity relationship. Intel. Lab. Syst. **10**, 213–227 (1991)
7. M. Randić, in *Topological Indices*, ed. by P.V.R. Schleyer, N.L. Allinger, T. Clark, J. Gasteiger, P.A. Kollman, H.F. Schaefer III, P.R. Schreiner The Encyclopedia of Computational Chemistry (Wiley, Chichester, 1998), pp. 3018–3032
8. J. Devillers, A.T. Balaban, *Topological Indices and Related Descriptors in QSAR and QSPR* (CRC Press, Boca Raton, FL, 2000)
9. N.L. Anderson, R. Esquer-Blasco, F. Richardson, P. Foxworthy, P. Eacho, The effects of peroxisome proliferations on protein abundances in mouse liver. Toxicol. Appl. Pharmacol. **137**, 75–89 (1996)
10. M. Randić, M. Novič, M. Vračko, On characterization of dose variations of 2-D proteomics maps by matrix invariants. J. Proteome Res. **1**, 217–226 (2002)
11. M. Randić, E. Estrada, Order from chaos: observing hormesis at the proteome level. J. Proteome Res. **4**, 2133–2136 (2005)
12. M. Randić, On graphical and numerical characterization of proteomics maps. J. Chem. Inf. Comput. Sci. **41**, 1330–1338 (2001)
13. M. Randić, J. Zupan, M. Novič, On 3-D graphical representation of proteomics maps and their numerical characterization. J. Chem. Inf. Comput. Sci. **41**, 1339–1344 (2001)
14. M. Randić, F. Witzmann, M. Vračko, S.C. Basak, On characterization of proteomivcs maps and chemically induced chanes in proteomes using matrix invariants: application to peroxisome proliferators. Med. Chem. Res. **10**, 456–479 (2001)
15. M. Randić, J. Zupan, M. Novič, B.D. Gute, S.C. Basak, Novel matrix invariants for characterization of changes of proteoics maps. SAR QSAR Environ. Res. **13**, 689–703 (2002)
16. M. Randić, N. Lerš, D. Vukičević, D. Plavšić, B.D. Gute, S.C. Basak, Canonical labeling of proteome maps. J. Proteome Res. **4**, 1347–1352 (2005)
17. M. Randić, A graph theoretical characterization of proteomics maps. Int. J. Quantum Chem. **90**, 848–858 (2002)
18. M. Randić, M. Novič, M. Vračko, D. Plavšić, Study of proteome maps using partial ordering. J. Theor. Biol. **266**, 21–28 (2010)
19. Ž. Bajzer, M. Randić, D. Plavšić, S.C. Basak, Novel map descriptors for characterization of toxic effects in proteomics maps. J. Mol. Graph. Model. **22**, 1–9 (2003)
20. M. Randić, N. Lerš, D. Plavšić, S.C. Basak, Characterization of 2-D proteome maps based on the nearest neighborhoods of spots. Croat. Chem. Acta **77**, 345–351 (2004)

21. M. Randić, M. Novič, M. Vračko, Novel characterization of proteomics maps by sequential neighborhood of protein spots. J. Chem. Inf. Model. **45**, 1205–1213 (2005)
22. M. Randić, N. Lerš, D. Plavšić, S.C. Basak, On invariants of a 2-D proteome map derived from neighborhood graphs. J. Proteome Res. **3**, 778–785 (2004)
23. M. Randić, R. Orel, On numerical characterization of proteomics maps based on partitioning of 2-D maps into Voronoi regions. J. Math. Chem. **49**, 1759–1768 (2011)
24. G. Voronoi, Nouvelles applications des paramètres continus à la théorie des forms quadratiques. J. Reine Angewandte Math. **133**, 97–178 (1907)
25. B. Delaunay, Sur la sphère vide. Izv. Akad. Nauk SSSR, Otdel. Mat. Estest. Nauk **7**, 793–800 (1934)
26. B.R. Kowalski, C.F. Bender, Pattern recognition. Powerful approach to interpreting chemical data. J. Am. Cem. Soc. **94**, 5632–5639 (1972)
27. P.F. Ash, E.D. Bolker, Generalized Dirichlet tessellations. Geometrie Dedicata **20**, 209–243 (1986)
28. L. Mu, WVD2009 (Multiplicatively weighted Voronoi diagram, computer program) http://www.ggy.uga.edu/people/faculty/mu/ (2009)